Hindawi
Journal of Chemistry
Volume 2023, Article ID 3481389, 15 pages
https://doi.org/10.1155/2023/3481389

Research Article

Green Synthesis, Characterization, and Antibacterial Activity of CuO/ZnO Nanocomposite Using *Zingiber officinale* Rhizome Extract

Elias Takele,[1] **Raji Feyisa Bogale**,[1] **Gemechu Shumi**,[1] **and Girmaye Kenasa**[2]

[1]*Department of Chemistry, College of Natural and Computational Sciences, Wallaga University, Nekemte 395, Ethiopia*
[2]*Department of Biology, College of Natural and Computational Sciences, Wallaga University, Nekemte 395, Ethiopia*

Correspondence should be addressed to Elias Takele; eliastakele41@gmail.com and Girmaye Kenasa; girmayek@gmail.com

Received 26 April 2023; Revised 14 July 2023; Accepted 31 July 2023; Published 11 August 2023

Academic Editor: Luca Conti

The synthesis of metal oxide nanocomposite by using the green method has gotten special consideration due to a cheaper and eco-friendly approach. Decreasing antibiotic effectiveness calls for the fast advancement of other alternative antimicrobials. CuO, ZnO, and CuO/ZnO nanocomposites were successfully synthesized using *Zingiber officinale* rhizome extract as a mild, renewable, and nontoxic reducing agent and proficient stabilizer with the nonappearance of hazardous and toxic chemicals. UV-Vis spectroscopy, Fourier transform infrared (FT-IR) spectroscopy, and X-ray diffraction (XRD) were used to characterize CuO, ZnO, and CuO/ZnO nanocomposites. The UV-Visible result showed the absorbance peak at 270 nm, 355 nm, 365 nm, and 370 nm corresponding to the characteristic band of CuO NPs, ZnO NPs, 10% CuO/ZnO, and 20% CuO/ZnO nanocomposites, respectively. FT-IR confirmed the nature of bonds and the presence of different functional groups in the *Zingiber officinale* rhizome extract, CuO, ZnO, and CuO/ZnO nanocomposites. The XRD analysis revealed that all the synthesized particles have a crystalline nature with a particle size of 4.35 nm, 14.54 nm, 18.41 nm, and 20.50 nm of CuO NPs, ZnO NPs, 10% CuO/ZnO, and 20% CuO/ZnO NCs, respectively. The synthesized nanoparticles and nanocomposites showed inhibition against Gram-positive and Gram-negative bacteria up to a concentration of 12.5 mg/mL. The highest inhibition against *Staphylococcus aureus* ATCC 25926 and *Escherichia coli* ATCC was 20 ± 0.7 mm and 16 ± 0.5 mm in diameter, respectively, by 50 mg/mL of 20% CuO/ZnO NCs. In general, the biosynthesized nanoparticles and nanocomposites showed effective antibacterial activity.

1. Introduction

Nanoscience and technology play a crucial part in numerous scientific fields with their particular features. Nanotechnology helps in reducing the particle size of materials as an efficient and reliable tool for enhancing their biocompatibility and can universally alter the view concerning science [1]. Nanoparticles are small particles made through nanotechnology. They have sizes from 1 to 100 nm [2]. The study of nanomaterials has greatly increased. They have unique qualities like being very hard, conducting electricity, staying chemically stable, having the ability to speed up chemical reactions, and fighting against microbial and antioxidants. Nanomaterials with the ability to kill microbial have been widely used in medicine [3].

The fast growth of industry and population greatly impacts the environment and raises many concerns and challenges about creating a sustainable and healthy ecosystem. Nanoparticles are tiny particles that are used to make the environment clean and safe. They help improve technology in industries [4]. Diseases that can be easily spread are a big danger to people everywhere. In the past few years, scientists have been using nanobiotechnology to create new drugs and find ways to control diseases [5]. Metal oxide nanoparticles are very important in nanotechnology because they are used a lot in different industries and pharmaceuticals. They are used as disinfectants, catalysts, fillers, and drugs that fight against bacteria [6]. Moreover, metal oxide nanomaterials have different reactions against microbes depending on their size [7].

Inorganic metal oxide nanoparticles are interesting because they are chemically stable, safe, and effective at killing bacteria [8]. Metal oxide nanoparticles have been used in many areas such as sensors, photocatalysts, protecting against UV rays, carrying drugs, making cosmetics, filling materials in medicine, and killing bacteria agents [9]. One of these metal oxides is zinc oxide nanoparticle (ZnO) as an n-type semiconductor. It is a special type of material that conducts electricity in a particular way. It has a lot of good qualities, like being environmentally friendly, cheap, very stable, and easy to prepare [10]. On the other hand, copper oxide nanoparticles (CuO) are considered another type of p-type semiconductor that is commonly used. They have low band gap energy, are chemically stable, friendly for the environment, and have properties that can reduce inflammation and antibacterial activities [11]. ZnO and CuO NPs are considered the most common nanoparticles because they have great chemical, physical, and mechanical properties. Some of these properties include a low melting temperature, a bigger surface area, structural stability, high diffusion, and high surface energy [12].

There are many expensive ways to synthesize CuO/ZnO nanocomposites using chemical and physical methods. These ways also involve using toxic organic solvents and hazardous reagents, high pressure, and risks to the environment and living things. Because of this, that restricts their use in medical applications [13]. There are several papers on the green synthesis of CuO, ZnO, and CuO/ZnO nanocomposite for use in biological applications utilizing plant extracts. Biological approaches have a number of advantages over chemical and physical ones for synthesizing metal oxide nanocomposite. Based on the previous literature reports, ZnO NPs, CuO NPs, and CuO/ZnO NCs have been synthesized from various plant extracts. The green synthesis of CuO NPs using the *Syzygium guineense (SyG)* leaf extract on bacteria with the evaluation of electrochemical properties has been reported [14]. The extract from the medicinal plant, *Syzygium guineense* leaf, was used to synthesize copper and its oxide (SyG-CuO) nanostructures, and the process was successful. The green copper oxide NPs showed great potential for antimicrobial and electrochemical applications.

ZnO nanoparticles were synthesized using a natural and environmentally friendly method using an extract from *Zingiber officinale* rhizome. The synthesized ZnO nanoparticles were incorporated into a glucose biosensor. The prepared biosensor exhibited good electrocatalytic ability for the determination of glucose [15]. In addition, ZnO nanoparticles were synthesized using the extract of *Ranunculus multifidus* plant. Therefore, the antibacterial activity of synthesized ZnO NPs was tested against Gram-negative and Gram-positive bacterial strains such as *Escherichia coli*, *Pseudomonas aeruginosa*, *Staphylococcus aureus,* and *Bacillus subtilis*. The finding showed that the synthesized ZnO NPs had a strong ability against bacterial strains, especially Gram-positive pathogenic bacterial strains [16]. However, the ZnO material has a large energy band gap as reported previously [17] which can decrease the antibacterial properties. The addition of CuO to ZnO could form the CuO/ZnO nanocomposite, which increases particle size and decreases the band gap energy [18]. CuO/ZnO nanocomposite was biosynthesized by mixing copper and zinc precursors with a type of fungus, *Penicillium corylophilum* strain, for photocatalytic activity. The synthesized CuO/ZnO nanocomposite has higher stability than either of the ZnO and CuO nanoparticles [19].

The ZnO and Cu-doped ZnO nanocomposites (NCs) were synthesized by the solution combustion synthesis (SCS) method, which is fast and saves energy, to synthesize the materials. The doping and heterojunction method made the properties of NCs better than just using the individual nanoparticles, and this increased the capabilities of the materials to transfer charge and absorb light better [20]. When two metal oxides are combined, they have some important characteristics, they are very stable when exposed to heat, and they have a large surface area. This helps them react better because they have more active sites on their surface and they work more effectively [21].

Many researchers have worked on green synthesis, characterization, and photocatalytic activities of nanocomposite. However, up to the knowledge of the authors, there is a gap in the synthesis of CuO/ZnO binary nanocomposites using *Zingiber officinale* rhizome extract. *Zingiber officinale* (ginger) is a medicinal plant; it belongs to the Zingiberaceae family. Ginger is a common spice that is used in many different countries, particularly in Asia and Africa [22]. Because *Zingiber officinale* rhizome contains a lot of phytochemicals, it is selected for the synthesis of CuO/ZnO NCs. Therefore, in this study, the CuO/ZnO nanocomposite is selected as the target material to be synthesized through a plant-mediated routine and to further investigate their antibacterial activity. CuO/ZnO nanocomposite exhibited enhanced antibacterial activity compared with single-component CuO and ZnO NPs. This study aims to address a lack of the synthesis of CuO/ZnO binary nanocomposites using the extracts from *Zingiber officinale* rhizome for enhanced antibacterial properties than single CuO and ZnO nanoparticles.

2. Materials and Methods

2.1. Chemicals and Reagents. All the chemicals and reagents used in this study were of analytical grade. Copper nitrate trihydrate (95%, Cu (NO_3) $2.3H_2O$), sodium hydroxide (99%, NaOH), zinc acetate dihydrate (98%, Zn (CH_3COO) $2.2H_2O$), ethanol (97%), iron chloride hexahydrated (97%, $FeCl_3.6H_2O$), hydrochloric acid (18%, HCl), sulphuric acid (98%, H_2SO_4), potassium Iodide (99%, KI), iodine (99%, I2), sodium chloride (99%, NaCl), dimethyl sulfoxide (99.5%, DMSO), muller hinton agar, erythromycin (15μg), *Zingiber officinale* rhizome extract, and deionized water were used in experiments.

2.2. Apparatus and Instruments. Oven, thermometer, mortar and pestle, digital balance, hot plate with magnetic stirrer (HLHM5-300W), refrigerator, centrifuge, centrifuge tubes, beakers (50, 100, 150, 250, and 600 mL), rack, droppers, quartz cuvettes, graduated cylinders (10, 25, 50, 100, and 250 mL), glass rode, erlenmeyer flasks (50, 100, 250,

and 500 mL), electrical grinder (Miller) (TW135), filter paper (Whatman No. 1), portable pH meter (PH-013), volumetric flasks (100, 500, and 1000 mL), and test tubes are apparatus used in this study. UV-Vis Spectroscopy (DU800R DRAWELL), X-ray diffractometer (XRD-7000 X-RAY DIFFRACTOMETER) (SHIMADZU Corporation (Japan)), and Fourier transform infrared spectrometry (FT-IR) (Perkin Elmer, 65) are instruments used for characterization.

2.3. Plant Material Collection and Identification. The rhizome of *Zingiber officinale* was purchased from Nekemte, Oromia region, East Wollega Zone, in March 2022. Then, it was identified and authenticated at the National Herbarium of Ethiopia, which is part of Addis Ababa University.

2.4. Preparation of Zingiber officinale Rhizome Extract. The *Zingiber officinale* rhizome was cleaned with tap water and then with distilled water to get rid of any dirt. It was dried and turned into a fine powder. Lastly, it was kept at room temperature for later use. 10 g of *Zingiber officinale* dried powder was mixed with 100 mL of double distilled water in a 250 mL Erlenmeyer flask, and a magnetic heater stirrer was used for stirring at 70°C for 30 min to get the extract. The obtained extract was then centrifuged at 6000 revolutions per minute and passed through a filter (Figure 1). The filtered extract was stored in a refrigerator at 4°C for future experimental use [23].

2.5. Phytochemical Screening of the Zingiber officinale Rhizome Extract. The qualitative phytochemical test was done using standard and previously reported steps to check various phytochemicals in the extract [24]. Phytochemical Screening of *Zingiber officinale* rhizome extract was done at Chemistry Laboratory, Wallaga University. Therefore, the presence of phytochemicals such as alkaloids, phenols, saponins, flavonoids, and tannins in the extract was checked (Table 1).

2.6. Optimization Methods for Green Synthesis of CuO, ZnO NPs, and CuO/ZnO NCs. Optimization is very important to obtain nanoparticles and nanocomposites with high quality, stability, and desired size. Based on previous reports, different parameters were adjusted as being optimum conditions for nanoparticle synthesis by changing one parameter and keeping the other constant at a time to get the optimum results. Therefore, the effects of metal salt concentration, the amount of *Zingiber officinale* extract, pH, and temperature were optimized [27].

2.7. Synthesis of the CuO NPs, ZnO NPs, and CuO/ZnO NCs Using the Aqueous Extract of Zingiber officinale Rhizome. CuO NPs, ZnO NPs, and CuO/ZnO NCs were synthesized using a method that had been described before with some improvement.

2.7.1. Synthesis of CuO Nanoparticles. Copper oxide nanoparticles were synthesized by using 0.1 M Cu $(NO_3)_2.3H_2O$ (Figure S1). In brief, 100 mL of the copper nitrate trihydrate was taken in a 250 mL Erlenmeyer flask and 25 mL of the *Zingiber officinale* rhizome extract was added slowly to reduce copper ions to its copper oxide nanoparticles. Then, 10 mL of 2 M NaOH solution was added to adjust pH to 11 while stirring it constantly. The solution was stirred continuously at 80°C for 2 h. The blue-colored solution turned green immediately and after about 2 h, a dark brown precipitate was formed. The dark brown precipitate formed indicated that all the copper ions have been reduced and CuO NPs have been formed [28]. The obtained precipitate was centrifuged at 10000 rpm for 10 min and washed several times using distilled water and ethanol for removal of impurities, and the sample was dried at 80°C for 2 h.

2.7.2. Synthesis of ZnO Nanoparticles. Zinc oxide nanoparticles were successfully synthesized using *Zingiber officinale* rhizome extracts (Figure S1). 0.1 M zinc (II) acetate dihydrate $(Zn\ (CH_3COO)_2.2H_2O)$ was prepared by adding 2.195 g of zinc (II) acetate dihydrate in 100 mL deionized water in a 250 mL beaker. 25 mL of *Zingiber officinale* rhizome extract was added and stirred for a few minutes. The pH of the solution was adjusted to 11 by using 2 M NaOH while stirring. Then, the solution was stirred continuously at 90°C for 2 h, and the white-colored precipitate was observed in the solution. The precipitate was collected and centrifuged at 10000 rpm for 10 min. Finally, the obtained precipitate was cleaned with deionized water and absolute ethanol several times, the precipitate was collected, dried in an oven at 90°C for 2 h, and ground to a powder by using mortar and pestle, and it was kept for further physical characterizations and biological applications [29].

2.7.3. Synthesis of CuO/ZnO Nanocomposites. CuO/ZnO nanocomposite has been successfully synthesized in an eco-friendly manner using *Zingiber officinale* rhizome extract. The same procedure was used for CuO and ZnO nanoparticles (Figure S1). For the synthesis of 20% CuO/ZnO nanocomposite, 1.76 g zinc (II) acetate dihydrate and 0.4832 g copper nitrate trihydrate were added to 100 mL deionized water and 25 mL of the *Zingiber officinale* rhizome extract. An aqueous solution of NaOH (2 M) was added drop-wise to adjust the pH of the solution to 11 and the formed precipitate was centrifuged at 10000 rpm for 10 min, and the precipitate was cleaned and dried in the same way as ZnO NPs [23]. In the synthesis of the 10% CuO/ZnO nanocomposite, 1.98 g of zinc acetate and 0.2416 g of copper nitrate were used (Figure 2).

2.8. Characterization of Green Synthesized CuO NPs, ZnO NPs, and CuO/ZnO NCs. The visual property of CuO NPs, ZnO NPs, and CuO/ZnO NCs was studied, by using UV-Vis absorption spectra from 200 to 800 nm range of wavelength. FT-IR was used to identify which functional groups are

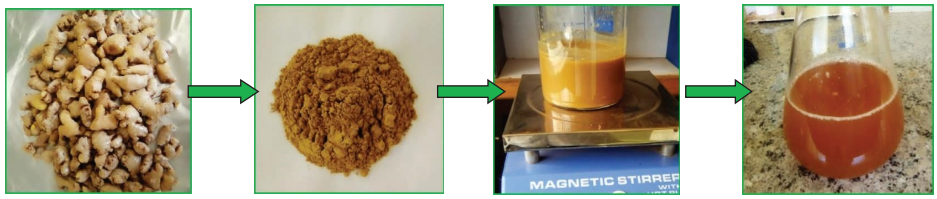

ZO rhizome | powder of ZO | Boiled at 70°C for 30 min | ZO aqueous extract

Figure 1: Schematic representation of extraction of *Zingiber officinale* rhizome.

involved in reducing the metal ions to nanoparticles and nanocomposites. The size, crystallinity, and purity of the nanoparticles and nanocomposites were characterized using XRD [30].

2.9. Antibacterial Activity of Green Synthesized CuO NPs, ZnO NPs, and Cu/ZnO NCs

2.9.1. Source of Test Organisms. The microorganisms that were used in this experiment were *Staphylococcus aureus ATCC 25926* and *Escherichia coli ATCC 25922*. The organisms were originally obtained from Ethiopia Public Health Institute and freeze-preserved in the Microbiology Laboratory, Wallaga University. The culture was activated in Muller–Hinton broth media at 37°C for 48 h on a rotary incubator shaker and spread-plated on selective and deferential agar media to check for viability and purity.

2.9.2. Antibacterial Activity Test. The test was done using Muller–Hinton agar media by the disc diffusion method. 1 mL of actively growing bacterial inoculums (from the logarithmic growth phase) that have approximately 10^7 CFU·mL^{-1} (colony forming units) (0.5 McFarland Standard) was uniformly spread using a swab on the agar media. The inoculated plates were put at room temperature for 6 min to allow for any surface moisture to be absorbed before applying the samples. Simultaneously, 50 mg·mL^{-1} of the green synthesized NPs and NCs was prepared in a 10% DMSO, and the autoclaved filter paper discs (diameter: 6 mm) were loaded with synthesized NPs and NCs. When the filter paper absorbed the green synthesized NPs and NCs, these were put on the Mueller–Hinton agar plates that had been inoculated. Erythromycin (15 μg) was used as the positive control, and a filter paper disc soaked with 10% DMSO was used as the negative control. The zones of inhibition were measured in mm after incubation of plates for 24 h at 37°C [31].

2.9.3. Minimum Inhibitory Concentration (MIC). The green synthesized nanoparticles and nanocomposites that showed a positive effect in a bacteria test for the disc diffusion were used to determine the minimum inhibitory concentration (MIC) by using the dilution method with little modification. Serial dilutions of the green synthesized nanoparticles and nanocomposites were prepared in the 10% DMSO with concentrations of 6.25, 12.50, 15, 25, and 50 mg/mL. Then, filter paper discs containing the samples at the desired concentration were placed on top of the agar surface. Generally, antimicrobial agents were diffused into the agar, and zones of inhibition were measured [32].

2.10. Data Analysis. The data related to antibacterial activities were done by using one-way ANOVA using statistical analysis software (SAS 14.1) at $\alpha = 0.05$.

3. Results and Discussion

3.1. Phytochemical Screening of Zingiber officinale (ZO) Rhizome Extract. In this study, *Zingiber officinale* (ZO) has been extracted by using deionized water and then the presence of its phytochemicals such as tannins, phenols, flavonoids, alkaloids, and saponins was tested. During synthesis, the phytochemicals found in the extract are used as the reducing agent to change metal ions to metal oxide nanoparticles and nanocomposites and simultaneously used as capping agents to protect the NP agglomeration. The results of the qualitative phytochemical analysis of the *Zingiber officinale* (ZO) extract are shown in Table 2. The result represented in Table 2 indicates the presence of flavonoids, phenols, alkaloids, and saponins confirming the availability of polyols which serve as the capping agent and reducing agent.

3.2. Synthesis of CuO, ZnO Nanoparticles, and CuO/ZnO Nanocomposites. The green method was applied to synthesize CuO, ZnO NPs, and CuO/ZnO NCs using *Zingiber officinale* rhizome extract. The phytochemicals found in the extract acted as reducing agents to reduce the metal ions to their corresponding nanoparticles. When the *Zingiber officinale* extract was added to blue copper nitrate, greenish color was formed; after 2 h of heating, dark brown solid (precipitate) formed indicating the formation of CuO nanoparticles. When the *Zingiber officinale* extract was added to colorless zinc acetate, a white precipitate was formed indicating the formation of ZnO nanoparticles. When the *Zingiber officinale* extract was added to the mixed solution of blue copper nitrate and zinc acetate, a light greenish blue precipitate was formed indicating the formation of CuO/ZnO NCs (Figure 3).

3.3. The Effects of Different Parameters on the Synthesis of CuO, ZnO, and CuO/ZnO NCs

3.3.1. Effect of Precursor Metal Salt Concentrations. To achieve an optimum condition for the synthesis of nanoparticles, the amount ratio of the plant extract should match with the concentration of metal precursors used [33].

Table 1: Qualitative tests for phytochemical screening of *Zingiber officinale* rhizome extract.

No	Phytochemicals	Tests	Procedures	Observations	References
1	Alkaloids	Mayer's reagent	A few drops of Mayer's reagent were added to 3 mL of filtrate (extract)	Formation of a creamy precipitate	[24]
2	Phenols	Ferric chloride	2 drops of 0.1% $FeCl_3$ were added to 4 mL of plant extract solution in a test tube	Formation of dark green solution	[25, 26]
3	Flavonoids	Alkaline reagent	3 mL of extract was reacted with 5 drops of NaOH solution in a test tube	Formation of yellow color, which disappears when some drops of dilute acid are added	[24]
4	Tannins	Ferric chloride	2 mL of distilled water was added to 3 mL of plant extract and then mixed with 3 drops of 1% $FeCl_3$ solution	Formation of a blue-black color	[25, 26]
5	Saponins	Froth test	3 mL of extract was mixed with 5 mL distilled water and shaken in a test tube for 15 min	The formation of a stable foam layer	[24]

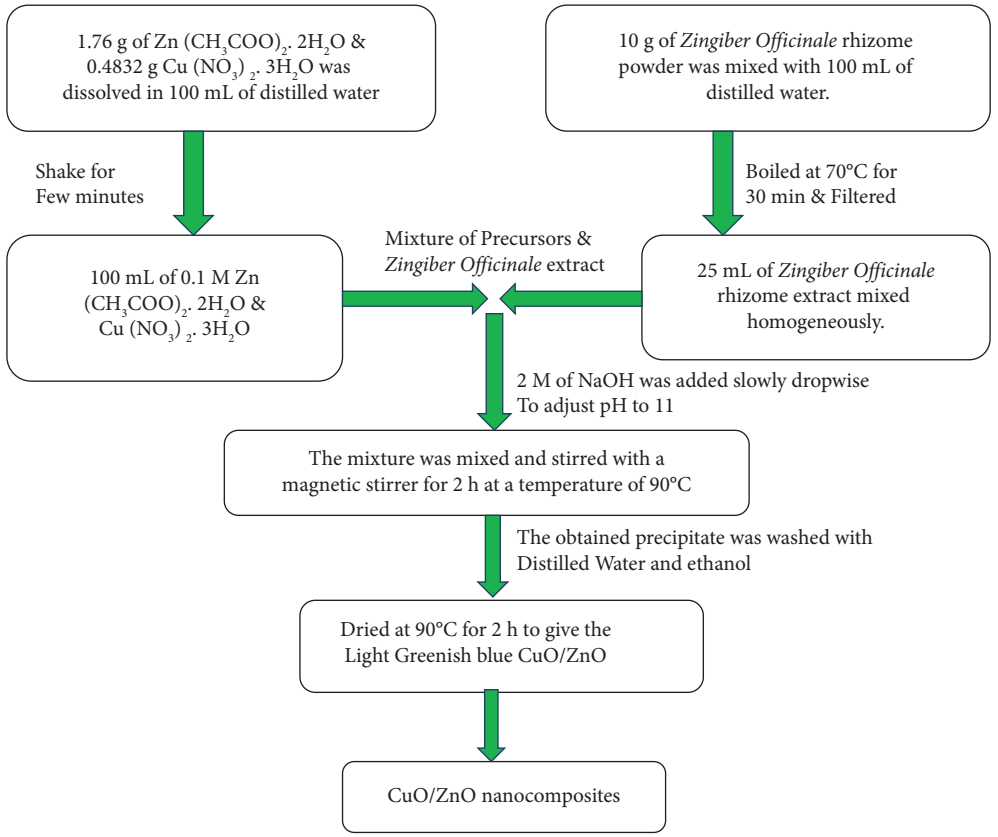

Figure 2: Synthesis of 20% CuO/ZnO NCs from zinc (II) acetate dihydrate and copper (II) nitrate trihydrate using *Zingiber officinale* rhizome extract.

Table 2: The results of phytochemical screening of *Zingiber officinale* rhizome extract.

Phytochemicals	Tests	Observations	Result
Alkaloids	Mayer's reagent test	Formation of a creamy precipitate	+
Phenols	Ferric chloride test	Dark green color	+
Flavonoids	Alkaline reagent test	Formation of yellow color, which disappeared when some drops of dilute HCl were added	+
Tannins	Ferric chloride test	Blue-black color	+
Saponins	Froth test	Formation of foam	+

The "+" sign indicates the presence of phytochemicals in the ZO extract.

Accordingly, 100 mL of metal precursor with different concentrations was used. So, 0.01, 0.03, 0.05, 0.1, and 0.2 M concentrations were used. As the concentration of the solution metal precursor was increased from 0.05 M to 0.1 M, the sharpness and intensity of the absorption peak were increased. However, when the metal precursor concentration was further increased to 0.2 M, the intensity of the absorption peak decreased. As a result, it was determined that further increasing the concentration of metal precursor more than the optimized value made a decrease in the yield in the synthesis of nanoparticles. This is likely due to the fact that the higher concentrations of Cu $(NO_3)_2$ and Zn $(CH_3COO)_2$ act in favor of agglomeration of the CuO and ZnO particles rather than in the formation of capped nanoparticles and nanocomposites in a colloidal solution [34]. Then, 0.1 M was taken as the optimum concentration for the synthesis of CuO, ZnO, and CuO/ZnO NCs.

3.3.2. Effect of Volume of Zingiber officinale Rhizome Extracts. The process of synthesis of NPs and NCs using plant extracts relies on the specific phytochemicals found in plant extracts and the amount used [35]. The amount of plant extracts used in the preparation of nanoparticles influences how long it takes to synthesize them. Previous report has found that using more extracts can speed up the synthesis process of nanoparticles. This is because there are more chemical ingredients available in the solution which binds with the precursor to synthesize nanoparticle form rapidly and stabilize them [36]. In this study, 10 mL, 15 mL, 20 mL, 25 mL, and 30 mL aqueous solutions of *Zingiber officinale* rhizome extract were used with 100 mL of 0.1 M precursor salt solutions. It was noticed that the absorption and peak prominence got better when the amount of extract increased from 10 mL to 25 mL. Then 25 mL was optimized because a sharp peak with high intensity was obtained.

(a) (b) (c)

Figure 3: Green synthesized (a) CuO NPs, (b) ZnO NPs, and (c) CuO/ZnO NCs using ZO extract.

When the volume was higher or smaller than this amount, the absorption peak was decreased. This shows that when the amount of extracts is higher, the biomolecules act as reducing agents and cap the nanoparticle surfaces preventing them from aggregation [37].

3.3.3. Effect of pH. The pH value measures how acidic or basic a solution is. The varying pH values of the solution influenced the synthesis of CuO and ZnO nanoparticles and CuO/ZnO nanocomposites. As previously reported, the pH level can greatly impact the size and texture of certain nanoparticles synthesized using plant extracts [33]. In addition, changes in pH levels have been used to control the shape and size of the synthesized nanoparticles [38]. The pH of the solution varied from 5 to 12. When the pH level of the solution was raised, the absorption peak of nanoparticles and nanocomposites increased. The characteristic absorption peak was obtained at pH 10 and 11, so pH 11 was optimized because a better peak and maximum absorption peak intensity were found at pH 11 with 25 mL of plant extracts. At pH 5-7, no absorption peaks were seen, indicating that the acidic pH is not good for efficient synthesis due to the slow reaction rate. At pH 12, the absorption peak was reduced due to NP aggregation, indicating that the basic pH of 11 is best for producing CuO/ZnO NCs and CuO and ZnO NPs [39].

3.3.4. Effect of Temperature. Temperature is an important factor that affects the synthesis of metal oxide nanoparticles. The temperature suggested for the biosynthesis of metal oxide nanoparticles is between 25°C and 100°C [40]. To identify the influence of temperature on the synthesis of CuO/ZnO NCs, ZnO, and CuO NPs, optimization was done at six different temperatures (room temperature, 50°C, 70°C, 80°C, 90°C, and 100°C) to obtain optimum temperature synthesis and keep the amount of the precursor constant (25 mL). 80°C for CuO NPs and 90°C were optimized for ZnO NPs and CuO/ZnO NCs. According to the results, the intensity of NP and NC absorbance peak increased with temperature. This observation may be due to the fact that at higher temperatures, the reduction of metal ions to its nanoparticles is rapid [39]. However, when further increased in temperature beyond the optimized value, the absorption peak became less intense. This observation may also be due to the agglomeration of the NPs and NCs, possibly because the heat destroyed the reducing agents and capping agents found in the plant extracts [39].

3.3.5. The Ratio of Precursors for Nanocomposite. To obtain the optimum ratio of CuO/ZnO, different amounts of the metal precursor solution were used. 10% (10 mL), 20% (20 mL), 30% (30 mL), 40% (40 mL), and 50% (50 mL) of 0.1 M of Cu $(NO_3)_2.2H_2O$ with 90 mL, 80 mL, 70 mL, 60 mL, and 50 mL of 0.1 M of Zn $(CH_3COO)_2.2H_2O$ were used, respectively. 10% and 20% were optimized because the absorption peak with high intensity and the largest wavelength was obtained at these ratios (Figure S2).

3.4. Characterization of Green Synthesized CuO NPs, ZnO NPs, and CuO/ZnO NCs

3.4.1. UV-Vis Absorption Spectral Analysis. UV-Visible spectroscopy characterization was done at the Department of Chemistry, Wallaga University. In addition to a color

change, the reduction of metal ions to nanoparticles and nanocomposites was confirmed by measuring the UV-Visible spectrum, for the detection of surface plasmon resonance (SPR) by taking a small amount of the synthesized sample and diluting it in deionized water. UV-Vis spectrum was measured in the wavelength range of 200–800 nm. An aqueous extract of the *Zingiber officinale* rhizome has been used to synthesize NPs and NCs.

The green synthesized CuO, ZnO, 10% CuO/ZnO, and 20% CuO/ZnO nanocomposites exhibited maximum absorption bands at 270 nm, 355 nm, 365 nm, and 370 nm, respectively (Figure 4). The result matches with values that were reported previously [41–43]. The addition of CuO NPs improved the energy band gap compared to ZnO NPs without the addition of any material. The value of the energy band gap was calculated using the Tauc equation [44]. The adsorption edges of the ZnO NPs were blue-shifted when compared to the wavelength of bulk ZnO which was seen at 385 nm [45]. The absorption peak shift towards blue was because of a decrease in the particle sizes for the ZnO NPs synthesized by using *Zingiber officinale* rhizome extract, and this change is due to the quantum confinement effect [46]. The energy band gaps were 1.65 eV, 2.90 eV, 2.76 eV, and 2.58 eV for CuO NPs, ZnO NPs, 10% CuO/ZnO, and 20% CuO/ZnO NCs, respectively (Figure 5). The band gap for ZnO-NPs is higher compared to CuO/ZnO NCs, which indicates that an increase in CuO amount in the nanocomposites results in a decrease in the energy band gap. On the other hand, *Zingiber officinale* rhizome extract shows a UV-Visible absorption peak of 275 nm in the ultraviolet region (Figure 4). This is in line with the previously reported value [23].

3.4.2. Fourier Transform Infrared (FT-IR) Spectroscopy Analysis. Phytochemicals that are responsible for capping, reduction, and stabilizing are identified by using FT-IR. FT-IR characterization was conducted at Addis Ababa University. The FT-IR peaks are assigned to the different functional groups of molecules found in the *Zingiber officinale* rhizome extract, nanoparticles, and nanocomposites [47]. FT-IR analysis was done to identify functional groups of biomolecules involved in the green synthesis of CuO, ZnO NPs, and CuO/ZnO NCs.

In this study, the identification of the functional groups in the *Zingiber officinale* rhizome extract and green synthesized nanocomposites was done using FT-IR spectroscopy (Figure 6), which confirmed that the *Zingiber officinale* rhizome extracts contain compounds bearing the -OH, C-H (due to aldehyde), C=O, -C-C, and -C-H (methyl) functional group because of the appearance of peaks at around 3233 (broad), 2930, 1622, 1391, 1107 (C-O), and 1047 cm^{-1} (C-OH). The broad -OH peak shows the presence of phenolic compounds, which is possibly responsible for the stabilization process of the nanoparticles. The carbonyl groups appeared to confirm that compounds such as ketones, esters, and aldehydes are present [48].

The FT-IR spectrum showed peaks at 3570, 3264, 1620, 1381, 1076, 937, and 693 cm^{-1} for CuO NPs, 3347, 1653, 1560,

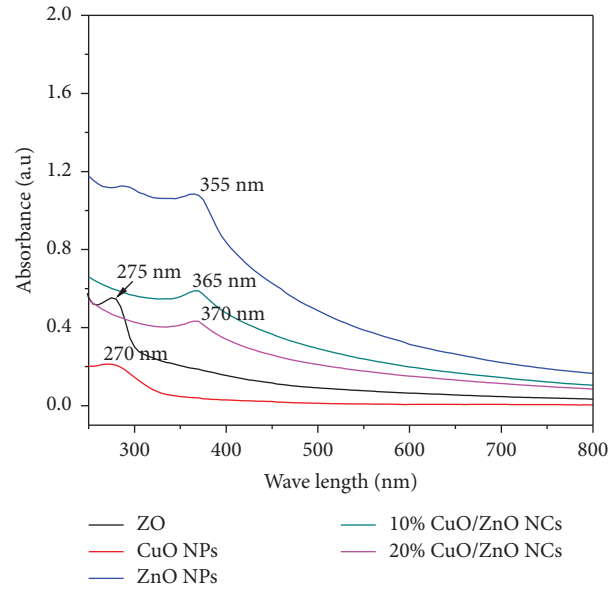

Figure 4: UV-Vis spectrum of ZO, CuO NPs, ZnO NPs, 10% CuO/ZnO, and 20% CuO/ZnO NCs.

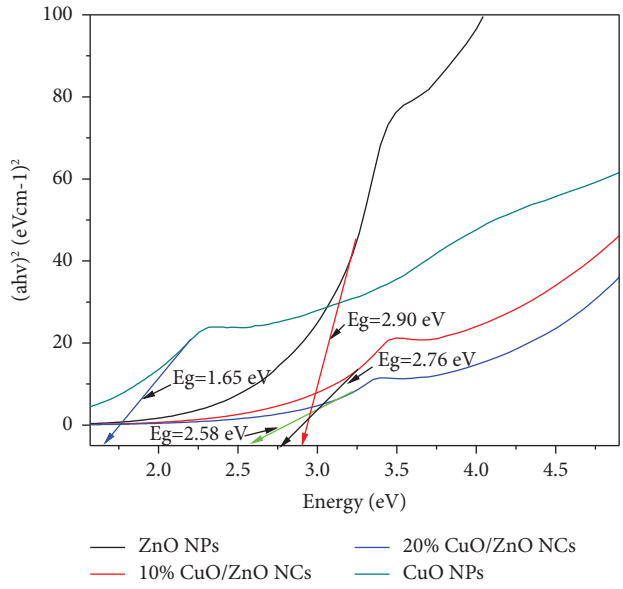

Figure 5: Energy band gap for CuO NPs, ZnO NPs, 10% CuO/ZnO, and 20% CuO/ZnO NCs.

1397, 1049, 860, and 691 cm^{-1} for ZnO NPs, 3345, 1645, 1580, 1395, 1045,841, and 649 cm^{-1} for 10% CuO/ZnO NCs, and 3356, 1647, 1559, 1395, 1042, and 841 cm^{-1} for 10% CuO/ZnO NCs (Figure 7). The peak at 3570 corresponds to the N-H stretching of amines, showing the involvement of amines in the stabilization of NPs and NCs [49]. The broad peaks at 3356, 3347, 3345, and 3264 cm^{-1} can be attributed to O-H stretching vibration. The presence of the -OH functional group suggests the presence of absorbed water on the surface of the synthesized nanoparticles and nanocomposites [50].

The characteristic peaks at 1620, 1645, 1647, and 1653 cm^{-1} can be assigned to C=C (carbonyl group)

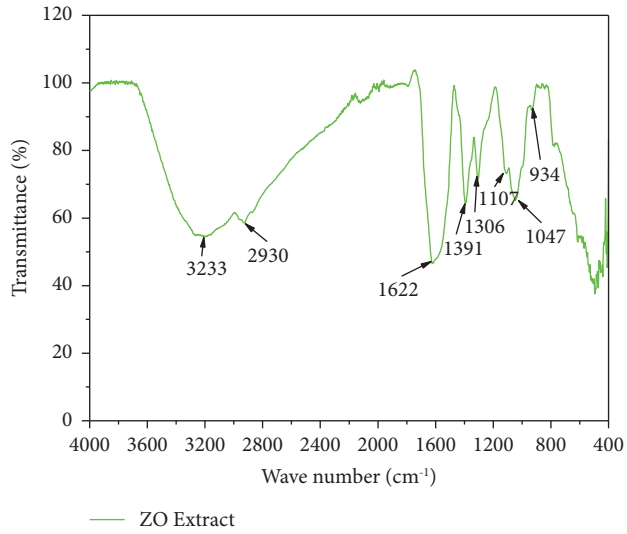

Figure 6: The FT-IR spectrum of *Zingiber officinale* rhizome extract.

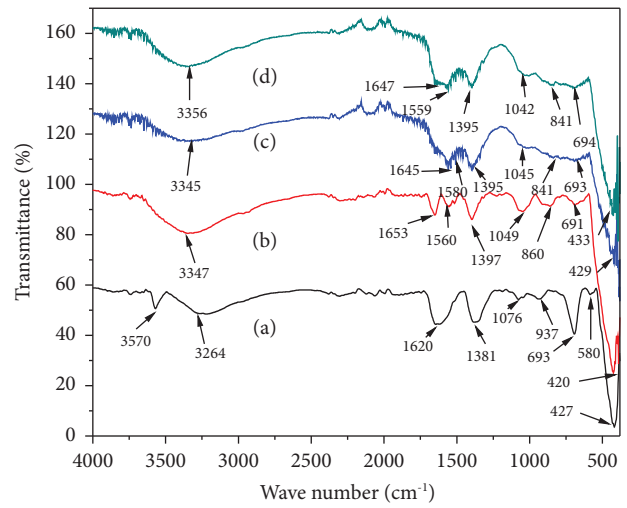

Figure 7: The FT-IR spectrum of green synthesized (a) CuO NPs, (b) ZnO NPs, (c) 10% CuO/ZnO NCs, and (d) 20% CuO/ZnO NCs using *Zingiber officinale* rhizome extract.

stretching. The absorption band at 1559, 1560, and 1580 cm^{-1} could be ascribed to amine-N-H stretching aromatic compounds corresponding to the biomolecules from ZO extract during the synthesis of samples. The broad absorption band at 1381, 1395, and 1397 cm^{-1} was attributed to the O-C-O stretching of esters or may be due to the C-H stretching vibration of the alkene group. The bands between 1042 and 1076 cm^{-1} are assigned to the stretching of C-O of phenols [51], whereas 937, 860, and 841 cm^{-1} may be assigned to C-H and C=C of the alkene [52].

The FT-IR spectra for the CuO, ZnO NPs, and CuO/ZnO NCs showed slight changes in some related peaks. The successful synthesis of Cu-O and Zn-O in all the samples was confirmed by the appearance of peaks at low wavelengths from 420 to 691 cm^{-1} [53]. The mode of vibration of Cu-O and Zn-O is in the range of 700–400 cm^{-1} [19]. FT-IR spectra of the green synthesized NPs and NCs showed slight changes in some related peaks and their intensities, indicating that the major biomolecules from the *Zingiber officinale* rhizome extract were capped or bound to the surface of CuO, ZnO, and CuO/ZnO NCs (Figure 7).

3.4.3. X-Ray Diffraction (XRD) Analysis. The size of green synthesized CuO NPs, ZnO NPs, 10% CuO/ZnO, and 20% CuO/ZnO NCs was characterized using XRD. The XRD was done at Adama Science and Technology University. All the peaks in the diffraction pattern at $2\theta \approx 35.5^{\circ}$, 36.45°, 38.96°, 42.75°, 48.81°, and 61.53° corresponding to the (002), (101), (111), (200), (202), and (220) crystal planes are well matched with the monoclinic phase of CuO. The 2θ values are in good agreement with the diffraction data card JCPDS-048-1548 confirming that CuO NPs have formed a crystalline in the monoclinic structure [54].

The diffraction peaks for ZnO NPs at $2\theta \approx 31.52^{\circ}$, 34.39°, 36.47°, 47.60°, 56.59°, 62.56°, 67.41°, and 69.78° belonging to (100), (002), (101), (102), (110), (103), and (201) crystal planes are well matched with the hexagonal wurtzite structure and fully consistent with the data from JCPDS No. 01-079-2205 [55]. The quality and intensity of peaks for ZnO NPs and CuO/ZnO NCs reflect the well crystalline nature of the nanostructures.

The absence of impurities is also reflected in the XRD pattern. The average crystalline size of CuO NPs, ZnO NPs, 10% CuO/ZnO, and 20% CuO/ZnO NCs obtained from full width at half maximum of diffraction is 4.35, 14.54, 18.41, and 20.50 nm, respectively. The intensities of peaks for ZnO NPs are higher compared to those for CuO NPs (Figure 8). This confirmed that ZnO NPs have a higher percentage in the CuO/ZnO NCs and are highly crystalline. The reason for the low peak intensities of CuO in CuO/ZnO is because of the coating role of ZnO NPs on CuO NPs [56].

The average crystallite size of each sample was calculated by using the Debye–Scherrer formula.

The average crystalline sizes of the CuO NPs obtained from the XRD data were between 1.05 nm and 9.29 nm, whereas for ZnO NPs, they were between 9.22 nm and 21.82 nm, for 10% CuO/ZnO, they were between 11.83 nm to 28.17 nm, and for 20% CuO/ZnO, they were between 16.16 nm to 31.82 nm (Table 3). Based on the XRD analysis, the average crystalline size of the CuO/ZnO increased as the ratio of CuO increased. This might be because the sizes of copper ions and zinc ions are different.

3.5. Antibacterial Activity of Green Synthesized CuO NPs, ZnO NPs, and CuO/ZnO NCs. Antibacterial activities of CuO NPs, ZnO NPs, 10% CuO/ZnO, and 20% CuO/ZnO NCs were tested for antibacterial activities starting from 50 mg/mL up to 6.25 mg/mL. As shown in Table 4, as the concentration of the NPs and NCs decreases, bacterial growth inhibition decreases for all samples and there was no inhibition at 6.25 mg/mL. The green synthesized nanoparticles and nanocomposites were active against both Gram-positive and Gram-negative bacteria using the disc diffusion method. The maximum growth inhibition was recorded by the 20%

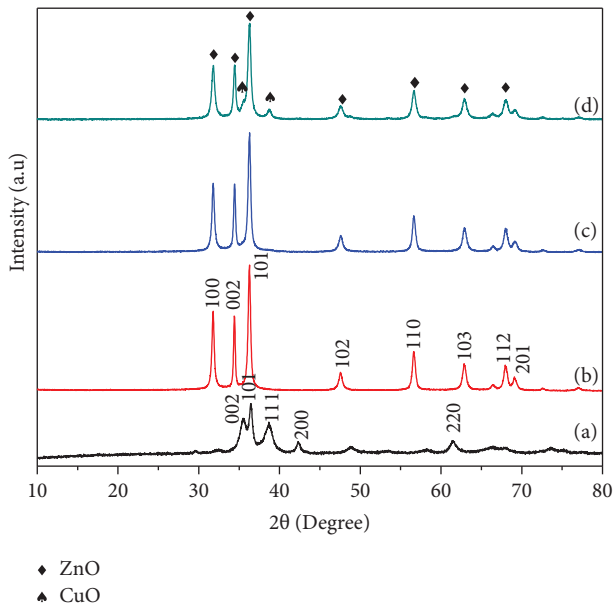

Figure 8: XRD spectrum of (a) CuO NPs, (b) ZnO NPs, (c) 10% CuO/ZnO, and (d) 20% CuO/ZnO NCs.

Table 3: XRD peak positions and crystalline size of CuO, ZnO, and CuO/ZnO NCs.

Samples	Miller indices (hkl)	2θ (degree)	FWHM (degree)	Crystallite size (nm)	Average crystalline size D (nm)
CuO NPs	002	35.50	1.11	7.51	4.35
	101	36.51	0.90	9.29	
	111	38.96	2.11	3.99	
	200	42.75	2.75	3.10	
	202	48.81	8.30	1.05	
	220	60.05	7.95	1.15	
ZnO NPs	100	31.52	0.48	16.66	14.54
	002	34.39	0.37	21.82	
	101	36.47	0.64	12.73	
	102	47.60	0.45	17.82	
	102	47.60	0.92	9.22	
	110	56.59	0.59	14.82	
	103	62.56	0.73	12.33	
	112	67.41	0.85	10.89	
	201	69.78	0.48	16.66	
10% CuO/ZnO NCs	100	31.28	0.37	21.75	18.41
	002	34.35	0.29	28.17	
	101	36.66	0.36	22.76	
	102	47.70	0.61	14.20	
	110	56.66	0.48	18.74	
	103	62.49	0.63	14.71	
	112	67.35	0.63	15.11	
	201	69.58	0.81	11.83	
20% CuO/ZnO NCs	100	31.14	0.35	23.53	20.5
	002	34.27	0.26	31.82	
	101	35.37	0.34	24.16	
	102	37.47	0.53	16.16	
	110	47.66	0.53	16.16	
	103	55.98	0.45	19.81	
	112	62.38	0.55	16.75	
	201	67.18	0.56	16.89	

Table 4: Comparative antibacterial activity of green synthesized CuO NPs, ZnO NPs, 10% CuO/ZnO, and 20% CuO/ZnO NCs.

Conc (in mg/mL)	Inhibition zone diameter (in mm)							
	CuO NPs		ZnO NPs		10% CuO/ZnO NCs		20% CuO/ZnO NCs	
	S. aureus	*E. coli*	*S. aureus*	*E. coli*	*S. aureus*	*E. coli*	*S. aureus*	*E. coli*
50	13 ± 0.6^{c}	12 ± 0.2^{c}	14 ± 0.1^{bc}	12 ± 0.2^{c}	15.5 ± 0.3^{b}	14.5 ± 0.5^{bc}	20 ± 0.7^{a}	16 ± 0.5^{b}
25	12 ± 0.3^{c}	11 ± 0.5^{cd}	10.5 ± 0.4^{cd}	11.5 ± 0.1^{cd}	13 ± 0.2^{c}	12 ± 0.4^{c}	19.5 ± 0.8^{a}	13 ± 0.7^{c}
15	9.5 ± 0.6^{d}	10 ± 0.3^{cd}	8.5 ± 0.9^{d}	9.5 ± 0.3^{d}	12 ± 0.1^{c}	10.5 ± 0.6^{cd}	17.5 ± 0.5^{ab}	11.5 ± 0.8^{cd}
12.5	8 ± 0.4^{d}	8 ± 0.4^{d}	0 ± 0.0	7.5 ± 0.1^{de}	10 ± 0.3^{cd}	10.5 ± 0.5^{cd}	13 ± 0.3^{c}	8 ± 0.9^{d}
6.25	$0 + 0$	$0 + 0$	$0 + 0$	$0 + 0$	$0 + 0$	$0 + 0$	$0 + 0$	$0 + 00$
Erythromycin (15 μg)	21.5 ± 0.7^{a}	18.5 ± 0.1^{ab}	21.5 ± 0.9^{a}	18.5 ± 0.2^{ab}	21.5 ± 0.6^{a}	18.5 ± 0.7^{ab}	21.5 ± 0.6^{a}	18.5 ± 0.7^{ab}
DMSO	0	0	0	0	0	0	0	0

In Table 4, values of the inhibition zone superscripted by the same letter both across the rows and columns are not significantly different from each other at $\alpha = 0.05$.

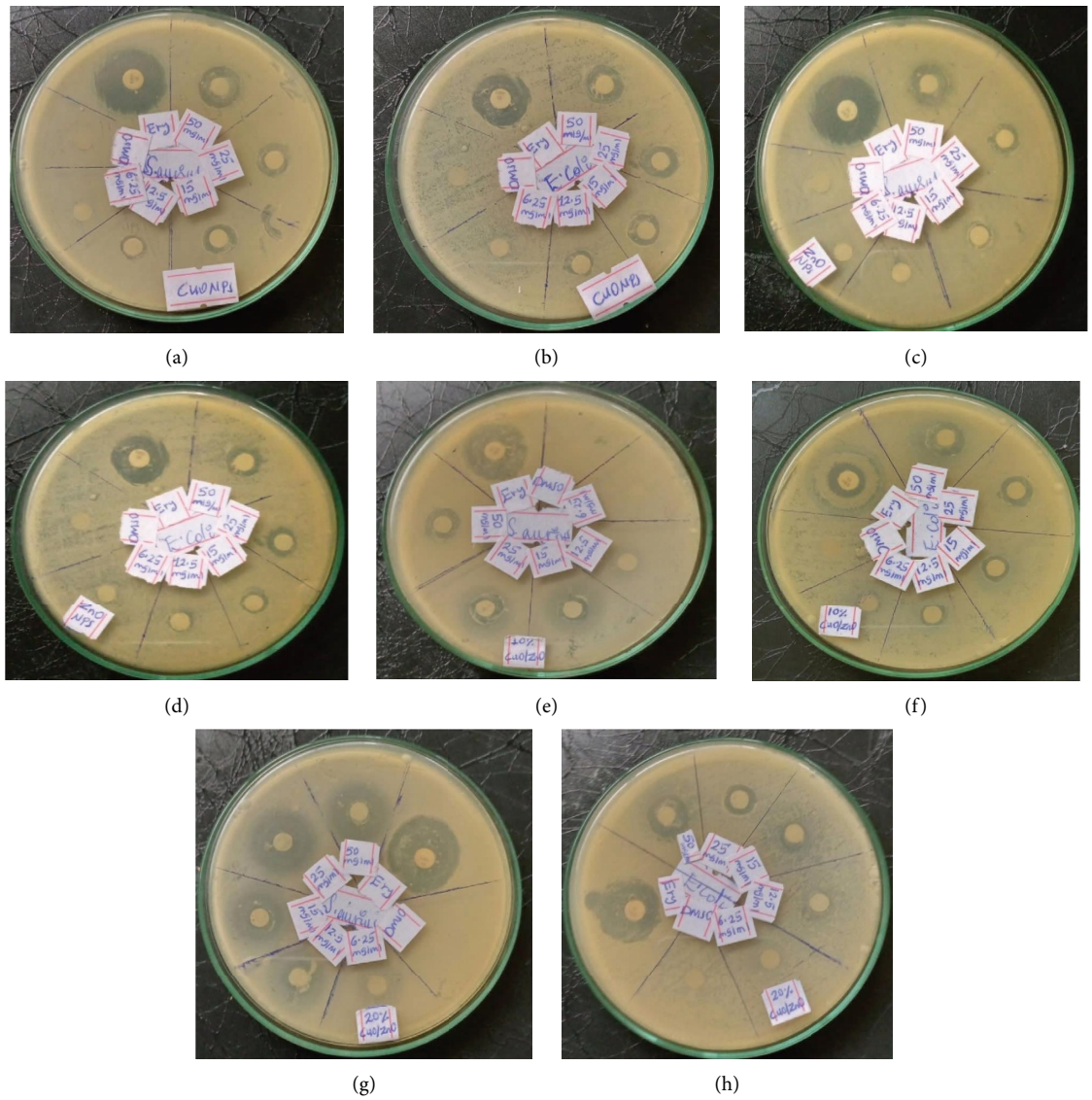

Figure 9: Inhibition zones of CuO NPs (a, b), ZnO NPs (c, d), 10% CuO/ZnO NCs (e, f), and 20% CuO/ZnO NCs (g, h) against S. aureus and E. coli, respectively.

CuO/ZnO NCs with inhibition of 20 mm and 16 mm on *S. aureus* ATCC 25926 and *E. coli* ATCC 25922, respectively, which is comparable to the inhibition of the strains by erythromycin (Table 4). The minimum growth inhibition of the NPs and NCs was 12.5 mg/mL on the two strains except for ZnO NPs on *S. aureus* which was 15 mg/mL. The

maximum inhibition was 13 mm on *S. aureus* at 12.5 mg/mL of 20% CuO/ZnO NCs (Table 4).

At all concentration levels for all the samples, the antimicrobial potential was strong on the Gram-positive strain (*S. aureus*) as compared to the Gram-negative bacteria (*E. coli*). But at 15 mg/mL, CuO NPs and ZnO NPs showed better effectiveness on *E. coli* than *S. aureus* (Table 4). At all concentrations, CuO NPs and ZnO NPs showed lower inhibition as compared to CuO/ZnO nanocomposite for both bacterial strains. This is because the combination of CuO and ZnO in the nanocomposite has a more free surface that can produce a higher amount of ROS compared to CuO and ZnO alone; adding CuO on ZnO produces more surface defect on CuO/ZnO. When the surface has more defects, it also has more ROS; this causes more bacteria to be prevented from growing [57].

From Table 4, it was concluded that the nanocomposites were found to be more effective at inhibiting the growth of Gram-positive bacteria compared to Gram-negative bacteria. This is because Gram-negative bacteria (*Escherichia coli*) typically contain thin cell walls and an outer membrane, which protects the inside of bacteria. The protective layer on the outside of the bacterial cell stops some drugs and antibiotics from getting inside. Gram-positive bacteria have a thick layer around their cells and a layer of the cytoplasmic membrane. This makes them easier to be killed by antibiotics compared to Gram-negative bacteria [58]. Gram-positive bacteria have thick cell walls that can absorb nanocomposites more than Gram-negative bacteria [59]. The most distinctive feature of Gram-positive bacteria is the thickness of its cell wall because a peptidoglycan layer is present [60]. When the energy band gap is smaller, the antibacterial activity increases because the electrons can move more easily from the valence band to the conduction band. The antibacterial activity of all samples further improved with increased concentration (Figure 9).

3.6. Possible Antibacterial Mechanism of Synthesized CuO, ZnO, and CuO/ZnO NCs. The NPs and NCs damage and kill bacteria and other microorganisms by producing ROS, breaking down the outer layers of their cells, and interfering with their proteins and DNA [61]. ROS are compounds that contain oxygen, and they are made up of highly unstable oxygen radicals such as superoxide ($O_2\bullet$), hydroxyl ($OH\bullet$), hydrogen peroxide (H_2O_2), and singlet oxygen (O_2) [62]. In this process, NPs can damage different microbial cell components by different mechanisms. CuO, ZnO, and CuO/ZnO NCs can harm different cell functions and harm cells and exert cytotoxicity, which makes them useful in stopping the growth of microbes (Figure S3).

Generally, CuO, ZnO NPs, and CuO/ZnO NCs destroy the bacterial cells by producing reactive oxygen species (ROS) and by changing or attaching to the natural components in metalloproteins [63].

4. Conclusions

The green and eco-friendly method was used to synthesize CuO/ZnO nanocomposites using *Zingiber officinale* rhizome extract as a reducing and stabilizing agent. A combination of two semiconductors could make the hybrid composites work better than just single material on its own. In this study, 10% CuO/ZnO and 20% CuO/ZnO nanocomposites, which have enhanced antibacterial activity than either of the CuO and ZnO nanoparticles, were green synthesized by using copper and zinc precursors with *Zingiber officinale* rhizome extract. UV-Vis, FT-IR, and XRD were used to investigate surface plasmon resonance (SPR), functional groups, and structure of samples. The UV-Vis absorption peaks indicate the formation of CuO, ZnO NPs, and CuO/ZnO NCs. FT-IR showed the presence of main functional groups in the synthesized samples. X-ray diffraction indicates the formation of the crystalline monoclinic structure of CuO NPs and the hexagonal structure of ZnO NPs and CuO/ZnO NCs. All synthesized NPs and NCs have shown good antibacterial activity on *S. aureus*. However, the 10% CuO/ZnO and 20% CuO/ZnO NCs revealed enhanced antibacterial activity than CuO NPs and ZnO NPs against both *S. aureus* and *E. coli*. This is due to the synergistic effect between the metal oxide nanoparticles in the nanocomposites. Generally, the result of this study indicates that synthesized NPs and NCs are more efficient against *S. aureus* compared to *E. coli*.

Data Availability

The data used in this study are available from the corresponding author upon request.

Conflicts of Interest

The authors declare that there are no conflicts of interest regarding the publication of this paper.

Authors' Contributions

Elias Takele was responsible for the concept, experiments, and manuscript preparation. Dr. Raji Feyisa and Dr. Girmaye Kenasa edited the manuscript. Besides, the antibacterial assay was conducted by Dr. Girmaye Kenasa. Gemechu Shumi participated in compiling and revising the manuscript. All authors have read and approved the final manuscript.

Acknowledgments

The authors are thankful to Wallaga University, Nekemte, Ethiopia.

Supplementary Materials

The scheme of the synthesis processes of CuO NPs, ZnO NPs, and CuO/ZnO NCs is shown in Figure S1. The optimized UV-Vis spectra of green synthesized ZnO NPs at various Zn $(CH_3COO)_2$ concentrations and pH, the effects of the volume of the extract, the pH of the CuO/ZnO NCs, and the temperature are shown in Figure S2. The possible way that CuO, ZnO, and CuO/ZnO NCs may kill bacteria is explained in Figure S3. (*Supplementary Materials*)

References

[1] T. Malik, G. Chauhan, G. Rath, R. S. R. Murthy, and A. K. Goyal, "Fusion and binding inhibition" key target for HIV-1 treatment and pre-exposure prophylaxis: targets, drug delivery, and nanotechnology approaches," *Drug Delivery*, vol. 24, no. 1, pp. 608–621, 2017.

[2] B. H. Abbasi, M. Shah, S. S. Hashmi et al., "Green bio-assisted synthesis, characterization, and biological evaluation of biocompatible ZnO NPs synthesized from different tissues of milk thistle (Silybummarianum)," *Nanomaterials*, vol. 9, no. 8, p. 1171, 2019.

[3] K. Varaprasad, M. López, D. Núñez et al., "Antibiotic copper oxide-curcumin nanomaterials for antibacterial applications," *Journal of Molecular Liquids*, vol. 300, pp. 112353–112423, 2020.

[4] W. Xie, Z. Zhang, L. Liao et al., "Green chemical mechanical polishing of sapphire wafers using a novel slurry," *Nanoscale*, vol. 12, no. 44, pp. 22518–22526, 2020.

[5] M. E. Villanueva, M. F. Ghibaudo, G. I. Tovar, G. J. Copello, and V. Campo Dall' Orto, "Oligomer-stabilized silver nanoparticles for antimicrobial coatings for plastics," *Nano-Structures & Nano-Objects*, vol. 24, pp. 100610–100622, 2020.

[6] M. M. Khan, S. F. Adil, and A. Al-Mayouf, "Metal oxides as photocatalysts," *Journal of Saudi Chemical Society*, vol. 19, no. 5, pp. 462–464, 2015.

[7] G. Sharmila, R. Sakthi Pradeep, K. Sandiya et al., "Biogenic synthesis of CuO nanoparticles using Bauhinia tomentosa leaves extract: characterization and its antibacterial application," *Journal of Molecular Structure*, vol. 1165, pp. 288–292, 2018.

[8] A. Rahman, M. H. Harunsani, A. L. Tan, and M. M. Khan, "Zinc oxide and zinc oxide-based nanostructures: biogenic and phytogenic synthesis, properties and applications," *Bioprocess and Biosystems Engineering*, vol. 44, no. 7, pp. 1333–1372, 2021.

[9] S. Ahmed, S. A. Chaudhry, S. A. Chaudhry, and S. Ikram, "A review on biogenic synthesis of ZnO nanoparticles using plant extracts and microbes: a prospect towards green chemistry," *Journal of Photochemistry and Photobiology B: Biology*, vol. 166, pp. 272–284, 2017.

[10] C. B. Ong, L. Y. Ng, and A. W. Mohammad, "A review of ZnO nanoparticles as solar photocatalysts: synthesis, mechanisms, and applications," *Renewable and Sustainable Energy Reviews*, vol. 81, pp. 536–551, 2018.

[11] I. Hussain, N. B. Singh, A. Singh, H. Singh, and S. C. Singh, "Green synthesis of nanoparticles and its potential application," *Biotechnology Letters*, vol. 38, no. 4, pp. 545–560, 2016.

[12] S. B. Mousavi and S. Zeinali Heris, "Experimental investigation of ZnO nanoparticles effects on thermophysical and tribological properties of diesel oil," *International Journal of Hydrogen Energy*, vol. 45, no. 43, pp. 23603–23614, 2020.

[13] R. Saleh and N. F. Djaja, "Transition-metal-doped ZnO nanoparticles: synthesis, characterization and photocatalytic activity under UV light," *Spectrochimica Acta Part A: Molecular and Biomolecular Spectroscopy*, vol. 130, pp. 581–590, 2014.

[14] T. Desalegn, H. C. A. Murthy, C. R. Ravikumar, and H. P. Nagaswarupa, "Green synthesis of CuO nanostructures using Syzygium guineense," *(Willd). DC Plant Leaf Extract and Their Applications. J Nanostruct*, vol. 11, no. 1, pp. 81–94, 2021.

[15] S. Dönmez, "Green synthesis of zinc oxide nanoparticles using ZingiberOfficinale root extract and their applications in glucose biosensor," *El-Cezeri Journal of Science and Engineering*, vol. 7, no. 3, pp. 1191–1200, 2020.

[16] T. Yilma, M. Kassaw, H. C. A. Murthy, and A. Dekebo, "ZnO nanoparticles synthesized using aerial extract of Ranunculus multifidus plant: antibacterial and antioxidant activity," *Journal of Nanomaterials*, vol. 2023, Article ID 8825762, 10 pages, 2023.

[17] A. M. M. Musa, M. Rasadujjaman, M. A. Gafur, A. T. M. K. Jamil, and M. K. Jamil, "Synthesis and characterization of dip-coated ZnO–CuO composite thin film for room-temperature CO2 gas sensing," *Thin Solid Films*, vol. 773, no. 2023, Article ID 139838, 2023.

[18] M. T. Qamar, M. Aslam, I. M. Ismail, N. Salah, and A. Hameed, "Synthesis, characterization, and sunlight-mediated photocatalytic activity of CuO-coated ZnO for the removal of nitrophenols," *ACS Applied Materials and Interfaces*, vol. 7, no. 16, pp. 8757–8769, 2015.

[19] A. Fouda, S. S. Salem, A. R. Wassel, M. F. Hamza, and T. I. Shaheen, "Optimization of green biosynthesized visible light active CuO/ZnO nano-photocatalysts for the degradation of organic methylene blue dye," *Heliyon*, vol. 6, no. 9, Article ID 04896, 2020.

[20] B. Abebe, D. Tsegaye, C. Sori, R. C. K. Renuka Prasad, and H. C. A. Murthy, "Cu/CuO-Doped ZnO nanocomposites via solution combustion synthesis for catalytic 4-nitrophenol reduction," *ACS Omega*, vol. 8, no. 10, pp. 9597–9606, 2023.

[21] V. Jayaraman and A. Mani, "Interfacial coupling effect of high surface area Pyrochlore like Ce2Zr2O7 over 2D g-C3N4 sheet photoactive material for efficient removal of organic pollutants," *Separation and Purification Technology*, vol. 235, Article ID 116242, 2020.

[22] D. Gao and Y. Zhang, "Comparative antibacterial activities of crude polysaccharides and flavonoids from Zingiberofficinale and their extraction," *American Journal of Tropical Medicine*, vol. 5, no. 6, pp. 235–238, 2010.

[23] M. Ali, M. Ijaz, M. Ikram, A. Ul-Hamid, M. Avais, and A. A. Anjum, "Biogenic synthesis, characterization and antibacterial potential evaluation of copper oxide nanoparticles against *Escherichia coli*," *Nanoscale Research Letters*, vol. 16, no. 1, p. 148, 2021.

[24] P. D. Sarda, A. D. Nagve, B. V. Salve, K. Prashar, and B. B. Warkhade, "Zingiberofficinale: phytochemical analysis and evaluation of antimicrobial activity in combination with commercial antibiotics," *International Journal of Current Research*, vol. 9, no. 10, pp. 59107–59111, 2017.

[25] P. Bazant, T. Sedlacek, I. Kuritka, D. Podlipny, and P. Holcapkova, "Synthesis and effect of hierarchically structured Ag-ZnO hybrid on the surface antibacterial activity of a propylene-based elastomer blends," *Materials*, vol. 11, no. 3, p. 363, 2018.

[26] S. Selvakumar, "Preliminary phytochemical investigation of various extracts of leaves of Kleiniagrandiflora," *American Journal of Pharmaceutical Research*, vol. 8, pp. 1277–1280, 2018.

[27] M. Nasrollahzadeh, S. M. Sajadi, A. Rostami-Vartooni, and S. M. Hussin, "Green synthesis of CuO nanoparticles using aqueous extract of Thymus vulgaris L. leaves and their catalytic performance for N-arylation of indoles and amines," *Journal of Colloid and Interface Science*, vol. 466, pp. 113–119, 2016.

[28] W. W. Andualem, F. K. Sabir, E. T. Mohammed, H. H. Belay, and B. A. Gonfa, "Synthesis of copper oxide nanoparticles using plant leaf extract of Catha edulis and its antibacterial

activity," *Journal of Nanotechnology*, vol. 2020, Article ID 2932434, 10 pages, 2020.

[29] A. M. Awwad, M. W. Amer, N. M. Salem, and A. O. Abdeen, "Green synthesis of zinc oxide nanoparticles (ZnO-NPs) using Ailanthus altissima fruit extracts and antibacterial activity," *International Journal of Chemistry*, vol. 6, no. 3, pp. 151–159, 2020.

[30] E. Gurgur, S. S. Oluyamo, A. O. Adetuyi, O. I. Omotunde, and A. E. Okoronkwo, "Green synthesis of zinc oxide nanoparticles and zinc oxide–silver, zinc oxide–copper nanocomposites using Brideliaferruginea as biotemplate," *SN Applied Sciences*, vol. 2, no. 5, pp. 911-912, 2020.

[31] M. H. N. De Zoysa, H. Rathnayake, R. P. Hewawasam, and W. M. D. Gaya Bandara Wijayaratne, "Determination of in vitro antimicrobial activity of five Sri Lankan medicinal plants against selected human pathogenic bacteria," *International Journal of Microbiology*, vol. 2019, Article ID 7431439, 8 pages, 2019.

[32] S. A. Khan, F. Noreen, S. Kanwal, A. Iqbal, and G. Hussain, "Green synthesis of ZnO and Cu-doped ZnO nanoparticles from leaf extracts of Abutilon indicum, Clerodendruminfortunatum, Clerodendruminerme and investigation of their biological and photocatalytic activities," *Materials Science and Engineering: C*, vol. 82, pp. 46–59, 2018.

[33] P. J. Jacob, M. J. Masarudin, M. Z. Hussein, and R. A. Rahim, "Optimization of process parameters influencing the sustainable construction of iron oxide nanoparticles by a novel tropical wetlands Streptomyces spp," *Journal of Cleaner Production*, vol. 232, pp. 193–202, 2019.

[34] P. Jamdagni, P. Khatri, and J. S. Rana, "Green synthesis of zinc oxide nanoparticles using flower extract of Nyctanthes arbortristis and their antifungal activity," *Journal of King Saud University Science*, vol. 30, no. 2, pp. 168–175, 2018.

[35] C. P. Devatha, K. Jagadeesh, and M. Patil, "Effect of Green synthesized iron nanoparticles by AzardirachtaIndica in different proportions on antibacterial activity," *Environmental Nanotechnology, Monitoring & Management*, vol. 9, pp. 85–94, 2018.

[36] M. Fazlzadeh, K. Rahmani, A. Zarei, H. Abdoallahzadeh, F. Nasiri, and R. Khosravi, "A novel green synthesis of zero-valent iron nanoparticles (NZVI) using three plant extracts and their efficient application for removal of Cr (VI) from aqueous solutions," *Advanced Powder Technology*, vol. 28, no. 1, pp. 122–130, 2017.

[37] S. Hashemi, Z. Asrar, S. Pourseyedi, and N. Nadernejad, "Green synthesis of ZnO nanoparticles by Olive (Olea europaea)," *IET Nanobiotechnology*, vol. 10, no. 6, pp. 400–404, 2016.

[38] S. Dubey and Y. C. Sharma, "Calotropisprocera mediated one pot green synthesis of cupric oxide nanoparticles (CuO NPs) for adsorptive removal of Cr (VI) from aqueous solutions," *Applied Organometallic Chemistry*, vol. 31, no. 12, p. 3849, 2017.

[39] M. M. Poojary, P. Passamonti, and A. V. Adhikari, "Green synthesis of silver and Gold nanoparticles using root bark extract of mammea suriga: characterization, process optimization, and their antibacterial activity," *BioNanoScience*, vol. 6, no. 2, pp. 110–120, 2016.

[40] J. K. Patra and K. H. Baek, "Green nanobiotechnology: factors affecting synthesis and characterization techniques," *Journal of Nanomaterials*, vol. 2014, no. 14, Article ID 417305, 12 pages, 2014.

[41] A. Shahpal, M. Aziz Choudhary, and Z. Ahmad, "An investigation on the synthesis and catalytic activities of pure and Cu-doped zinc oxide nanoparticles," *Cogent Chemistry*, vol. 3, no. 1, Article ID 1301241, 2017.

[42] R. Mohammadi-Aloucheh, A. Habibi-Yangjeh, A. Bayrami, S. Latifi-Navid, and A. Asadi, "Green synthesis of ZnO and ZnO/CuO nanocomposites in Mentha longifolia leaf extract: characterization and their application as anti-bacterial agents," *Journal of Materials Science: Materials in Electronics*, vol. 29, no. 16, pp. 13596–13605, 2018.

[43] S. Jayakodi, R. Shanmugam, B. O. Almutairi et al., "Azadirachtaindica-wrapped copper oxide nanoparticles as a novel functional material in cardiomyocyte cells: an ecotoxicity assessment on the embryonic development of *Danio rerio*," *Environmental Research*, vol. 212, Article ID 113153, 2022.

[44] A. Senapati, R. G. Gray, L. J. Middleton et al., "PROSPER: a randomised comparison of surgical treatments for rectal prolapse," *Colorectal Disease*, vol. 15, no. 7, pp. 858–868, 2013.

[45] S. R. Senthilkumar and T. Sivakumar, "Green tea (Camellia sinensis) mediated synthesis of zinc oxide (ZnO) nanoparticles and studies on their antimicrobial activities," *International Journal of Pharmacy and Pharmaceutical Sciences*, vol. 6, no. 6, pp. 461–465, 2014.

[46] K. Elumalai, S. Velmurugan, S. Ravi, V. Kathiravan, and S. Ashokkumar, "RETRACTED: green synthesis of zinc oxide nanoparticles using Moringa oleifera leaf extract and evaluation of its antimicrobial activity," *Spectrochimica Acta Part A: Molecular and Biomolecular Spectroscopy*, vol. 143, pp. 158–164, 2015.

[47] S. Azizi, R. Mohamad, R. A. Rahim et al., "ZnO-Ag core shell nanocomposite formed by green method using essential oil of wild ginger and their bactericidal and cytotoxic effects," *Applied Surface Science*, vol. 384, pp. 517–524, 2016.

[48] J. Osuntokun, D. C. Onwudiwe, and E. E. Ebenso, "Aqueous extract of broccoli mediated synthesis of CaO nanoparticles and its application in the photocatalytic degradation of bromocrescol green," *IET Nanobiotechnology*, vol. 12, no. 7, pp. 888–894, 2018.

[49] N. Thamer, N. Muftin, and S. Al-Rubae, "Optimization properties and characterization of green synthesis of copper oxide nanoparticles using aqueous extract of Cordia myxa L. Leaves," *Asian Journal of Chemistry*, vol. 30, no. 7, pp. 1559–1563, 2018.

[50] D. Saravanakkumar, S. Sivaranjani, K. Kaviyarasu et al., "Synthesis and characterization of ZnO–CuO nanocomposites powder by modified perfume spray pyrolysis method and its antimicrobial investigation," *Journal of Semiconductors*, vol. 39, no. 3, Article ID 033001, 2018.

[51] S. Alamdari, M. SasaniGhamsari, C. Lee et al., "Preparation and characterization of zinc oxide nanoparticles using leaf extract of Sambucusebulus," *Applied Sciences*, vol. 10, no. 10, p. 3620, 2020.

[52] H. Selim, A. Nada, and M. Eid, "The effect of ZnO and its nanocomposite on the performance of dye-sensitized solar cells," *Nanoscience and Nanotechnology*, vol. 12, p. 122, 2018.

[53] M. Patel, S. Mishra, R. Verma, and D. Shikha, "Synthesis of ZnO and CuO nanoparticles via Sol gel method and its characterization by using various technique," *Discover Materials*, vol. 2, no. 1, pp. 1–11, 2022.

[54] Y. H. Hsueh, P. H. Tsai, and K. S. Lin, "pH-dependent antimicrobial properties of copper oxide nanoparticles in *Staphylococcus aureus*," *International Journal of Molecular Sciences*, vol. 18, no. 4, p. 793, 2017.

[55] D. Dereje, G. Guta, and G. Birkinesh, "Synthesis of Ag-ZnO nanocomposite using PsidiumGuajava leaf extract and

evaluation of its photocatalytic activity," 2021, https://repository.ju.edu.et//handle/123456789/5842.

[56] Y. Cao, H. A. Dhahad, M. A. El-Shorbagy et al., "Green synthesis of bimetallic ZnO–CuO nanoparticles and their cytotoxicity properties," *Scientific Reports*, vol. 11, no. 1, pp. 23479–23488, 2021.

[57] T. Jan, S. Azmat, Q. Mansoor et al., "Superior antibacterial activity of ZnO-CuO nanocomposite synthesized by a chemical Co-precipitation approach," *Microbial Pathogenesis*, vol. 134, Article ID 103579, 2019.

[58] X. Zeng and J. Lin, "Beta-lactamase induction and cell wall metabolism in Gram-negative bacteria," *Frontiers in Microbiology*, vol. 4, p. 128, 2013.

[59] J. Pasquet, Y. Chevalier, E. Couval et al., "Antimicrobial activity of zinc oxide particles on five micro-organisms of the Challenge Tests related to their physicochemical properties," *International Journal of Pharmaceutics*, vol. 460, no. 1-2, pp. 92–100, 2014.

[60] M. Naseer, U. Aslam, B. Khalid, and B. Chen, "Green route to synthesize Zinc Oxide Nanoparticles using leaf extracts of Cassia fistula and Melia azadarach and their antibacterial potential," *Scientific Reports*, vol. 10, no. 1, pp. 9055–9061, 2020.

[61] L. Wang, C. Hu, and L. Shao, "The antimicrobial activity of nanoparticles: present situation and prospects for the future," *International Journal of Nanomedicine*, vol. 12, pp. 1227–1249, 2017.

[62] J. N. Moloney and T. G. Cotter, "ROS signaling in the biology of cancer," *Seminars in Cell & Developmental Biology*, vol. 80, pp. 50–64, 2018.

[63] Y. Fu, F. M. J. Chang, and D. P. Giedroc, "Copper transport and trafficking at the host–bacterial pathogen interface," *Accounts of Chemical Research*, vol. 47, no. 12, pp. 3605–3613, 2014.